

# Test on bifacial cells utilizing various ground surfaces

Daniela Fontani<sup>1</sup>, Paola Sansoni<sup>1</sup> and David Jafrancesco<sup>1</sup>, Luca Mercatelli<sup>1</sup>

<sup>1</sup> CNR-National Institute of Optics, Firenze (Italy)

## Abstract

The bifacial photovoltaic module (Bifacial PV) is a PV panel that can generate energy from both sides. This work studies different configurations of bifacial photovoltaic fields. Diffusing and retro-reflective (RR) materials are used to exploit the light reflected from the ground. So, the radiation not reaching the modules is minimized. The research includes ray tracing simulations of the possible ground configurations and field measurements on a small-scale system. Field measurements were developed to evaluate the effective contribution of the optimized fields to the production of electricity. The configurations measured in the field are compared in order to evaluate the actual increase in production compared to the classic photovoltaic (PV) module, which has only one active face. The studied configurations allow to increase the obtained peak power of more than 10 %.

*Keywords: Bifacial PV, Retro-Reflective (RR) Materials, Ray Tracing Simulations, Field Measurements.*

---

## 1. Introduction

Bifacial modules are acquiring an ever-greater space within the photovoltaic market and in the strategies of the main manufacturers. The bifacial photovoltaic module (Bifacial PV) is a particular type of panel that manages to generate energy from both sides of the photovoltaic cell, thus increasing production compared to a standard photovoltaic module (PV) (Guerrero-Lemus et al., 2016; Kopecek and Libal, 2021). A comprehensive review was carried out to present a detailed analysis of the thermal and electrical performance of bifacial photovoltaic technology (Gu et al 2020). It has been reported in the literature that the use of bifacial panels can improve the energy yield of power plants by 25-30% (Stein et al., 2021). The increase in production that a double-sided module can guarantee, thanks to the capture of the light reflected from the ground on the rear side, is a highly appreciated advantage in applications involving large ground systems, for which the payback times are still today the most important aspect. For this reason, it is necessary to install components capable of guaranteeing high electricity production and better performance.

A thorough investigation (Rodríguez-Gallegos et al., 2018) into the economic advantages of bifacial solar panels compared to monofacial panels has shown that bifacial panels are generally more cost-effective in areas with high ground reflectivity. Due to their promising efficiency, bifacial panels have been widely deployed in a variety of applications, such as green roofs, agriculture and highways (Sultan Mahmud et al., 2018; Riaz et al., 2021; Katsikogiannis et al., 2021; Baumann et al., 2019). A miniaturized test array was set up, as a commercial bifacial PV system using a 3×3 module array, for the systematic measurements of bifacial systems in various mounting conditions (Nussbaumer et al., 2019).

In bifacial modules it is important to consider the albedo of the ground. Albedo, i.e. the fraction of solar radiation reflected by a surface (Frezza et al., 2021), is a well investigated characteristic of the ground that can affect the power output of the bifacial photovoltaic modules. In this framework, the purpose is to identify suitable materials, to be deposited on the ground under and around the modules, in order to reduce the part of radiation not exploited by the modules, which would therefore be lost. In Riedel-Lyngskær et al 2021 the effect of spectral albedo in bifacial photovoltaic performance was analyzed.

In the literature there are articles with tests performed on photovoltaic solar fields that consider soils with grass (Bembe et al., 2018) and standard materials, like white paint (Riedel-Lyngskær et al., 2020) or concrete (Bembe et al., 2018), or discuss tests on roofs always using standard materials (Medium Brown Shingles, White Tiocoat/Swarco Beads, Aluminum Paint) (Sciara et al., 2016). A study was carried out on a commercial solar power plant in Seville,

where different vegetal species were planted in two strings, and the performance of the string was monitored (Rodriguez-Pastor et al., 2023).

The objective of this work is to confirm that the design of a bifacial photovoltaic field optimized for the exploitation of the light reflected from the ground is effective. In Fontani et al 2023, after having identified the materials that optimize the reflection towards the panels, to be deposited on the ground under and around the modules, the best configurations from an optical point of view were studied. In this way the part of radiation which does not impinge on the modules, and which would therefore not be utilized, is minimized. The work considered the following aspects: identification of suitable materials for the optimization of the collected light, optical simulations of the possible configurations, field measurements on a small-scale system. Field measurements were developed to evaluate the effective contribution of the optimized fields to the production of electricity. In this paper, the configurations measured in the field are compared in order to evaluate the actual increase in production compared to the classic photovoltaic (PV) module, which has only one active face.

## 2. Identification of materials and configurations of the fields

As a first step of the research, materials suitable for increasing the retro-reflected flux from the ground have been identified (Fontani et al., 2023). The retro-reflective panels used were made with a highly reflective white paint, to which glass beads with an average diameter of  $200 \div 300 \mu\text{m}$  were applied. The glass particles were dispersed as homogeneously as possible on the upper side of the panel itself. Four panels were realized to be used in the field experiments. A photo of these four panels with retro-reflective materials is shown in Fig. 1.



**Fig. 1: The four retroreflective panels used in the measurements.**

Furthermore, optical simulations were carried out to identify the best ground configurations in order to maximize the flux received by the bifacial module. From these studies, the most promising solutions resulted from those with a field made of diffusing-Lambertian soil and with a mixed configuration: mainly made up of diffusing-Lambertian soil with a part of the soil, the one behind the photovoltaic mini-modules, with retro-reflecting (RR) materials. A more extensive description of this process of material selection and optical simulation is presented in Fontani et al. (2023).

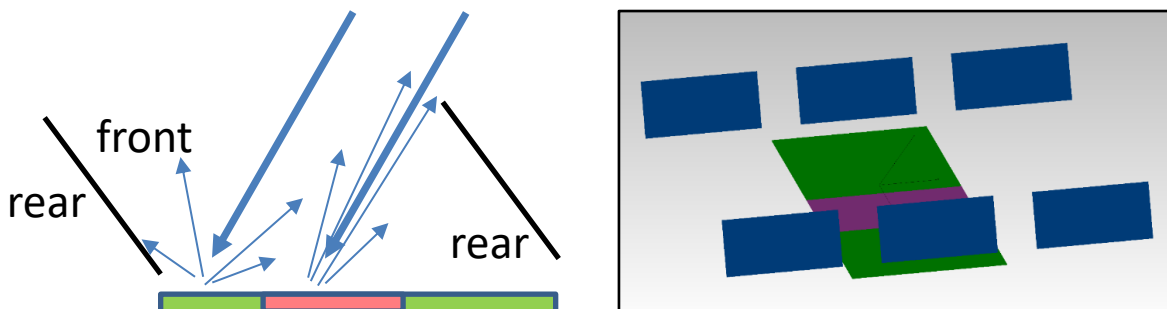


Fig. 2: The proposed mixed solution. Sketch of lateral view (left) and simulation 3D view (right). The green color indicates the ground with diffusing material, while the pink color shows the ground with RR material.

### 3. Measurements in the field

To verify the results of the simulations, some field measurements were carried out with direct exposure to the sun. Minimodules made up of 4 bifacial photovoltaic cells were used. The three different configurations examined for the field in which the measurements were carried out are:

- **Optimized Mixed field**, with diffusing material and retro-reflecting material,
- **Optimized field with diffusing material**,
- **Non-optimized field** (Reference field).

For the Optimized field with diffusing material and the Optimized Mixed field, several panels with diffusing paint and 4 panels with retro-reflective materials were made to be placed on the ground (Fig. 3).

For each measurement session of the Optimized Fields, the diffusive panels were placed on the ground so as to cover the entire surface. Furthermore, for the measurements with retro-reflective materials a retro-reflective panel was placed in the position foreseen in the simulations. The Non-optimized field measurements were carried out both without intervening on the measurement field, made up of gray stone, and by carrying out a measurement placing on the ground a sheet of black cardboard (Fig. 4).

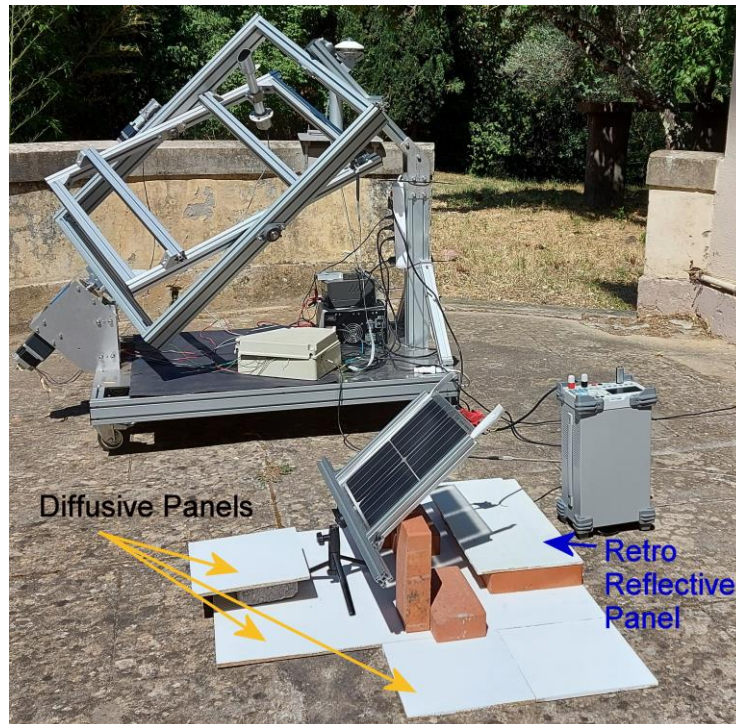
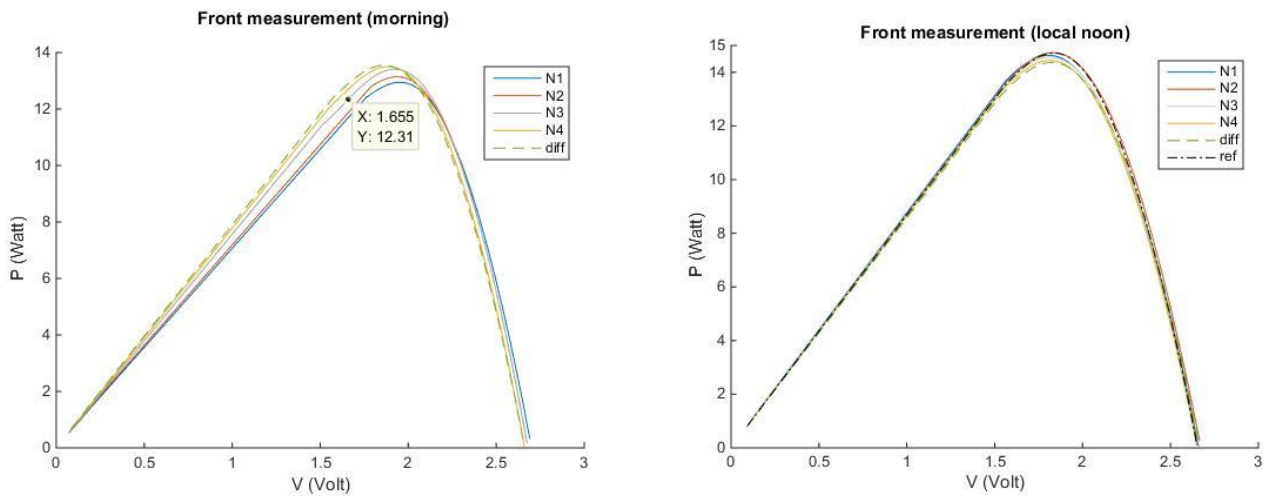


Fig. 3: Set-up of the field for the measurements.

Fig. 4: Set up of the Reference field measurement.

For each measurement session, the data are acquired initially considering only the side exposed to direct radiation (*Front*), obscuring the rear side of the minimodule (*Back*) with a covering. Then the covering was removed so that the minimodule works in a double-sided way (indicated with *Front+Back*). The Front configuration simulates the behavior of a classical PV module and is used for the comparison with the Bifacial configuration (*Front+Back*).

For each measurement session, the following were acquired: total radiation with a pyranometer and direct radiation with a pyrhelimeter; 3 sampling cycles of the voltage-current curve (VI) using a variable load; temperature of the cells at the beginning and at the end of the measurement session; ambient temperature at the beginning and at the end of the measurement session; open circuit voltage ( $V_{oc}$ ) at the beginning and at the end of the measurement session.



#### 4. Processing of measures

The VI data (voltage-current curve) acquired during the measurement sessions were interpolated to obtain the maximum power ( $P_{max}$ ) and obtain the short-circuit current value ( $I_{sc}$ ).

Fig. 5: Power versus Voltage graphs. Left: Front measurements performed in the morning. Right: Front measurement performed around the local noon.

The results of the elaboration for the Front measurement are plotted in the graphs shown in Figure 5. The curves report the values of the calculated power as a function of the voltage values. The curves indicated with N1, N2, N3 and N4 refer to measurements with Optimized Mixed field, obtained by alternating the 4 retro-reflecting panels.

While the curve indicated with “diff” is obtained placing on the ground only diffusive panels. The black curve in the right graph (called “ref”) is the reference measurement made using the black panel and the configuration shown in Figure 4.

Table 1 presents the values related to the graphs shown in Figure 5 and reports the data for the Front measurements performed in the morning and around the local noon.  $V_{oc}$  is the voltage measured in open circuit configuration,  $I_{sc}$  and  $P_{max}$  are the results of the interpolations.  $V_{oc}$  is express in Volt, the short-circuit current  $I_{sc}$  in Ampere and the maximum power  $P_{max}$  in Watt.

**Table 1: numerical data of the measurements shown in Figure 5.**

| Field configuration                            | Morning  |          |           | Local noon |          |           |
|--|----------|----------|-----------|------------|----------|-----------|
|  | $V_{oc}$ | $I_{sc}$ | $P_{max}$ | $V_{oc}$   | $I_{sc}$ | $P_{max}$ |
| <b>Optimized Mixed field</b> with panel N1     | 2,70     | 7,28     | 12,94     | 2,66       | 8,98     | 14,63     |
| <b>Optimized Mixed field</b> with panel N2     | 2,68     | 7,461    | 13,14     | 2,67       | 8,89     | 14,73     |
| <b>Optimized Mixed field</b> with panel N3     | 2,68     | 7,63     | 13,41     | 2,65       | 8,91     | 14,56     |
| <b>Optimized Mixed field</b> with panel N4     | 2,66     | 7,88     | 13,50     | 2,65       | 8,85     | 14,44     |
| <b>Optimized field with diffusing material</b> | 2,66     | 8,02     | 13,55     | 2,66       | 8,73     | 14,37     |
| Reference configuration (non-optimised)        |          |          |           | 2,65       | 8,83     | 14,71     |

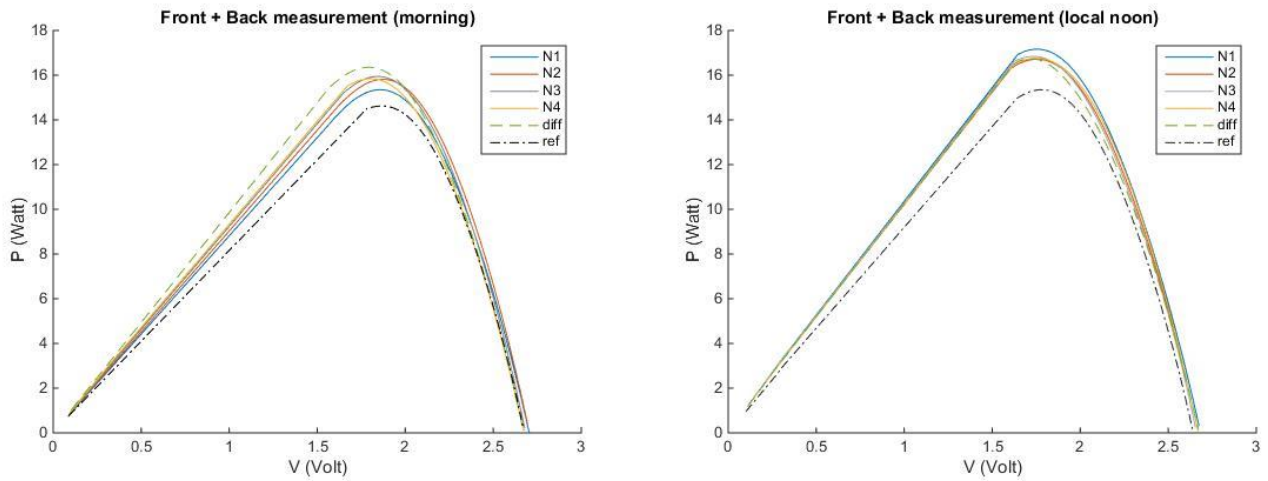


**Fig. 6: Power versus Voltage graphs. Left: Front+Back measurements performed in the morning. Right: Front+Back measurement performed around the local noon.**

The results of the elaboration for the Front+Back measurement are plotted in the graphs shown in Figure 6. The curves report the values of the calculated power as a function of the voltage values. Similarly, to Figure 5, the graphs indicated with N1, N2, N3 and N4 refer to measurements with Optimized Mixed field obtained by alternating the 4 retro-reflecting panels. While the curve indicated with “diff” is obtained placing on the ground only diffusive panels. The black curve (called “ref”) in the right plot of Figure 6 refers to the reference measurement made with the black panel and the configuration shown in Figure 4; while the black curve called “ref” in the left graph is obtained from a measurement in our data base, which was performed without using the black panel, so the ground was made of grey stone. The values related to the Front+Back measurements performed in the morning and around the local noon are reported in Table 2.  $V_{oc}$  is the voltage measured in open circuit configuration,  $I_{sc}$  and  $P_{max}$  are the results of the interpolation. Table 2 also reports the value of the average solar irradiance during the measurement,  $G_k$ , this quantity will be used for further elaborations.  $V_{oc}$  is expressed in Volt,  $I_{sc}$  in Ampere,  $P_{max}$  in Watt,  $G_k$  in Watt/m<sup>2</sup>.

**Table 2: numerical data of the measurements shown in Figure 6.**

| Field configuration                        | Morning  |          |           |       | Local noon |          |           |       |
|--|----------|----------|-----------|-------|------------|----------|-----------|-------|
|  | $V_{oc}$ | $I_{sc}$ | $P_{max}$ | $G_k$ | $V_{oc}$   | $I_{sc}$ | $P_{max}$ | $G_k$ |
| <b>Optimized Mixed field</b> with panel N1 | 2,70     | 8,95     | 15,35     | 853   | 2,68       | 10,86    | 17,16     | 985   |



|  |      |       |       |     |      |       |       |     |
|--|------|-------|-------|-----|------|-------|-------|-----|
| <b>Optimized Mixed field with panel N2</b>     | 2,70 | 9,09  | 15,81 | 889 | 2,67 | 10,74 | 16,71 | 970 |
| <b>Optimized Mixed field with panel N3</b>     | 2,68 | 9,36  | 15,94 | 892 | 2,66 | 10,92 | 16,84 | 987 |
| <b>Optimized Mixed field with panel N4</b>     | 2,67 | 9,60  | 15,84 | 909 | 2,67 | 10,76 | 16,75 | 995 |
| <b>Optimized field with diffusing material</b> | 2,67 | 10,02 | 16,35 | 929 | 2,67 | 10,71 | 16,74 | 978 |
| Reference configuration (non-optimized)        | 2,67 | 8,63  | 14,62 | 889 | 2,64 | 9,70  | 15,35 | 967 |

Since the irradiance value varies during outdoor measurements, for each measurement it was calculated the value of

$$m_k = P_k / G_k \quad (\text{eq. 1})$$

where  $P_k$  is the maximum power obtained in the interpolation of the k-th measurement, and  $G_k$  is the average solar irradiance during the measurement itself.

For each set of measurements, a reference value was chosen, and the following value was calculated:

$$\mu_k = (m_k - m_{ref}) / m_{ref} \quad (\text{eq. 2})$$

where the subscript “k” refers to the value of the k-th measurement and the subscript “ref” to the reference measurement.

Note that for constant irradiance the value of  $\mu_k$  is equivalent to the quantity  $\Delta P_{kmax}$ , calculated as:

$$\Delta P_{kmax} = (P_k - P_{ref}) / P_{ref} \quad (\text{eq.3})$$

The comparisons between the configurations were made based on the  $\Delta P_{kmax}$  and  $\mu_k$  values.

## 5. Comparison of measurements

Comparison 1: comparing the performance of a Bifacial module using different field configurations.

The first comparison is performed in order to understand the improvement given by the optimized grounds with respect to the non-optimized ground. The reference measurement, with non-optimized ground, for the local noon case is the measurement performed at noon with black sheets on the ground (these values are in Table 2). Since the measurement with the black panel is not available for the morning case, the reference data set for the morning has been chosen from our database, selecting a suitable configuration without modification of the ground and with the irradiance nearest to the mean value registered during the morning session (these values are in Table 2).

Table 3: Comparison between the various Bifacial (Front+Back) measurements.

| Field configuration                               | Morning               |             | Local noon            |             |
|---|-----------------------|-------------|-----------------------|-------------|
|   | $\Delta P_{kmax}$ (%) | $\mu_k$ (%) | $\Delta P_{kmax}$ (%) | $\mu_k$ (%) |
| <b>Optimized Mixed field with panel N1</b>        | 4,98%                 | 9,41%       | 11,82%                | 9,77%       |
| <b>Optimized Mixed field with panel N2</b>        | 8,15%                 | 8,15%       | 8,89%                 | 8,55%       |
| <b>Optimized Mixed field with panel N3</b>        | 9,04%                 | 8,68%       | 9,72%                 | 7,50%       |
| <b>Optimized Mixed field with panel N4</b>        | 8,36%                 | 5,98%       | 9,16%                 | 6,08%       |
| <i>Average of the 4 mixed fields measurements</i> | 7,63%                 | 8,05%       | 9,89%                 | 7,98%       |
| <b>Optimized field with diffusing material</b>    | 11,86%                | 7,04%       | 9,08%                 | 7,85%       |

Referring to mixed field measurements, since the production process is still at the laboratory level, in Table 3 there is also an average value of the measurements with the 4 retro-reflecting panels. The results show that the process for realizing the Retro Reflective panels needs still to be improved. These results indicate that the use of an optimized ground produces an advantage in the performances during all day, not only for the time where the optimized configuration has been calculated (local noon). The values of  $\mu_k$  result more stable than  $\Delta P_{kmax}$  that is influenced by

the variations of solar irradiance. The optimal field was obtained for the noon configuration; the values of  $\Delta P_{kmax}$  for local noon confirm that the average value of the Mixed field is better than the results obtained with ground composed only of diffusing materials, as expected. Meanwhile, the values of the normalized parameter  $\mu_k$  show a more constant behavior during the day and a better performance for the mixed solution. In fact, the mean values of  $\mu_k$  for the Retro Reflecting material are greater than the corresponding values obtained with the diffusing materials. While the mean value of the power of the field ( $\Delta P_{kmax}$ ) with Retro Reflective panels is greater than the power with only the diffusive material, but only at the local noon.

Comparison 2: comparing the performance of a standard PV module without optimized ground with a Bifacial Module with optimized ground.

Table 4 illustrates the values of the comparison between the performance of the single-sided cell and the performance of the double-sided cell. The single-sided cell is equivalent to the measurements carried out on the *Front* side only of a double-sided cell. The measurement on the double-sided cell has the contribution of the *Front+Back* sides of the minimodule. The reference measurement (*ref*) used in eq. 3 and eq. 2 for the calculation of  $\Delta P_{kmax}$  and  $\mu_k$  corresponds to the *Front* measure with the black cardboard.

In Table 4 the first four values (rows 2-5) refer to measurements with field in mixed configuration obtained by alternating the 4 retro-reflecting panels (indicated with N1-N4). Referring to these measurements, since the production process is still at the laboratory level, in Table 4 (row 6) there is also an average value of the measurements with the 4 retro-reflecting panels. Finally, the measurement in row 7 of Table 4 refers to the configuration with a field composed only of diffusing panels. For each measurement, the table reports the values of  $\Delta P_{kmax}$  and  $\mu_k$  calculated with eq. 3 and eq. 2. The last row reports the comparison between PV minimodule and Bifacial PV minimodule, for the reference configuration, which is with the non-optimized field.

Tab. 4: Comparison between the performance of PV minimodule and Bifacial PV minimodule at local noon.

| Field configuration                               | $\Delta P_{kmax}$ | $\mu_k$       |
|---|-------------------|---------------|
| <b>Optimized Mixed field</b> with panel N1        | 16,63%            | 15,21%        |
| <b>Optimized Mixed field</b> with panel N2        | 13,57%            | 13,92%        |
| <b>Optimized Mixed field</b> with panel N3        | 14,44%            | 12,82%        |
| <b>Optimized Mixed field</b> with panel N4        | 13,85%            | 11,34%        |
| <i>Average of the 4 mixed fields measurements</i> | <i>14,62%</i>     | <i>13,32%</i> |
| <b>Optimized field with diffusing material</b>    | 13,77%            | 13,19%        |
| Reference configuration (non-optimised)           | 4,30%             | 4,95%         |

Analyzing the results of Table 4 it can be noticed that both the optimized fields (Optimized Mixed field and Optimized field with diffusing material) give an improvement more than 10% with respect to the PV single face module. The bifacial configuration with non-optimized field gives an improvement of 4,30% for  $\Delta P_{kmax}$  and of 4,95% for  $\mu_k$ , so the addition of the optimized field boosts the value of around 10% for  $\Delta P_{kmax}$  and around 8% for  $\mu_k$ .

Since the amount of solar irradiance does not change in the raytracing simulations, the value of  $\Delta P_{kmax}$  and  $\mu_k$  in the simulations results the same. It is possible to evaluate the maximum amount of  $\Delta P_{kmax}$  (Fontani et al., 2023), because the power obtained on the receiver does not take into account the angular response of the Bifacial PV minimodule. This means that the expected  $\Delta P_{kmax}$ , calculated as the ratio between the recovered power of each configuration and the Direct Flux on the panel, was estimated to have a maximum of 17.7% for the Optimized field with diffusing material and 20.3% for the Optimized Mixed field. Hence, the results obtained show that is possible to recover the 2/3 of the power that reaches the back of the Bifacial Panel.

## 6. Conclusion

The purpose of this work is to find materials and field configurations to optimize the efficiency of the bifacial photovoltaic minimodules through the optimization of the solar field. This article presents an innovative approach trying to maximize the sun power collected by the back side of a bifacial PV module, performing a study on suitable materials and ray tracing simulations.

In a previous work (Fontani et al., 2023) some suitable Retro-Reflective (RR) materials have been studied and

realized to minimize the flux lost because it does not reach the rear part of the panel and maximize the recovery of the solar flux. It was found that the optimal RR material is the one with a diameter of microspheres of 200-300  $\mu\text{m}$  regardless of density. For the field optimization, a ray tracing analysis was performed in order to obtain the best configuration considering a real field and the materials examined in the previous study, both diffusive and RR. As a result of these simulations the best configuration is a mixed ground with diffusive parts and a RR part. The RR part is located in an area behind the photovoltaic panel. Some tests on a scaled field with a single minimodule were performed in order to verify the effectiveness of the optimizations combining the results of material studies and raytracing simulations. The measurement was executed in the summer season, 2 sets of measurements were performed on the same PV module alternating the 4 RR panels realized and the diffusive one. Moreover, a measurement with a black panel in a grey ground was done as reference for the noon measurement. The comparison between the measurements performed with and without the plywood panels on the ground shows that there is an improvement of the minimodule output when the ground is properly settled.

Comparing the performance of a Bifacial module using different field configurations it can be noticed that the values of  $\mu_k$  result more stable than  $\Delta P_{kmax}$  that is influenced by the variations of solar irradiance. The values of  $\Delta P_{kmax}$  for local noon confirm that the average value of the Mixed field is better than the results obtained with ground composed only of diffusing materials (this result was obtained from the simulations optimizing the field for the local noon). Meanwhile, the values of the normalized parameter  $\mu_k$  show a more constant behavior during the day and a constant better performance for the mixed solution.

Comparing the performance of a standard PV module (*Front* measurement) without optimized ground with a Bifacial Module (*Front+Back* measurement) with optimized ground it can be noticed that the bifacial configuration with non-optimized field causes an improvement of 4,30% for  $\Delta P_{kmax}$  and of 4,95% for  $\mu_k$ , while the addition of the optimized field boosts the value of around 10% for  $\Delta P_{kmax}$  and around 8% for  $\mu_k$ .

Utilizing the data of the raytracing simulation it is possible to affirm that the results obtained show that it is possible to recover the 2/3 of the power that reaches the back of the Bifacial Panel.

## 7. Acknowledgements

The present experimental research was funded by the Italian Ministry of University and Scientific Research (MUR) under the PON Project entitled "BEST4U-Bifacial Efficient Solar Cell Technology with 4-Terminal Architecture for Utility Scale".

## 8. References

- Baumann, T., Nussbaumer, H., Klenk, M., Dreisiebner, A., Carigiet, F., Baumgartner, F., 2019. Photovoltaic systems with vertically mounted bifacial PV modules in combination with green roofs. *Solar Energy* 190, 139–146. Issn: 0038092X. doi: 10.1016/j.solener.2019.08.014.
- Bembe, M. T., Chowdhury, S. P. D., Meeding, N., Lekhuleni, E. G., Ayanna M. B., Simelane, S., 2018. Effects of Grass and Concrete Reflective Surface on the Performance of Dual Axis Bifacial Solar PV Systems *IEEE PES/IAS PowerAfrica* 734-738, doi: 10.1109/PowerAfrica.2018.8521143.
- Frezza, L., Santoni, F., Piergentili, F., 2022. Sun direction determination improvement by albedo input estimation combining photodiodes and magnetometer, *Acta Astronautica*, 190, 134-148, doi:10.1016/j.actastro.2021.09.029.
- Fontani, D., Jafrancesco, D., Sansoni, P., Nicolini, A., Di Giuseppe, A., Pazzaglia, A., Castellani, B., Rossi, F., Mercatelli, L. 2023. Field optimization for bifacial modules. *Optical Materials*, 138, 113715. <https://doi.org/10.1016/j.optmat.2023.113715>.
- Guerrero-Lemus, R., Vega, R., Kim, T., Kimm, A., Shephard, L.E., 2016. Bifacial solar photovoltaics – A technology review, *Renewable and Sustainable Energy Reviews* 60, 1533-1549 <https://doi.org/10.1016/j.rser.2016.03.041>.
- Gu, W., Ma, T., Ahmed, S. Zhang, Y., Peng, J., 2020. A comprehensive review and outlook of bifacial photovoltaic (bPV) technology, *Energy Conversion and Management*, 223, 113283, doi:10.1016/j.enconman.2020.113283.
- Katsikogiannis, O.A., Ziar, H., Isabella, O., 2022. Integration of bifacial photovoltaics in agrivoltaic systems: A synergistic design approach. *Applied Energy* 309, 118475. Issn: 03062619. Doi: 10.1016/j.apenergy.2021.118475.
- Kopecek, R., Libal, J., 2021. Bifacial Photovoltaics 2021: Status, Opportunities and Challenges. *Energies* 14, 2076. <https://doi.org/10.3390/en14082076>.



- Nussbaumer, H., Klenk, M., Morf, M., Keller, N., 2019. Energy yield prediction of a bifacial PV system with a miniaturized test array, *Sol. Energy*. Doi:10.1016/j.solener.2018.12.042
- Riaz, M. H., Imran, H., Younas, R., Butt, N.Z., 2021. The optimization of vertical bifacial photovoltaic farms for efficient agrivoltaic systems. *Solar Energy* 230, 1004–1012. Issn: 0038092X. doi: 10.1016/j.solener.2021.10.051.
- Riedel-Lyngskær, N., Poulsen, P.B., Jakobsen, M.L., Nørgaard, P., Vedde, J., 2020. Value of bifacial photovoltaics used with highly reflective ground materials on single-axis trackers and fixed-tilt systems: a Danish case study. *IET Renew. Power Gener.* 14, 3946-3953. <https://doi.org/10.1049/iet-rpg.2020.0580>.
- Riedel-Lyngskær, N., Ribaconka, M., Pó, M., Thorseth, A., Thorsteinsson, S., Dam-Hansen, C., Jakobsen, M.L., 2022. The effect of spectral albedo in bifacial photovoltaic performance, *Solar Energy*, 231, 921-935, [doi:10.1016/j.solener.2021.12.023](https://doi.org/10.1016/j.solener.2021.12.023).
- Rodríguez-Gallegos, C.D., Bieri, M., Gandhi, O., Singh, J.P., Reindl, T., Panda, S.K., 2018. Monofacial vs bifacial Si-based PV modules: Which one is more cost-effective?. *Solar Energy* 176, 412–438. Issn: 0038092X. doi: 10.1016/j.solener.2018.10.012.
- Rodriguez-Pastor, D.A., Ildefonso-Sanchez, A.F., Soltero, V.M., Peralta, M.E., Chacartegui, R., 2023. A new predictive model for the design and evaluation of bifacial photovoltaic plants under the influence of vegetation soils, *Journal of Cleaner Production*, 385, 135701, [doi:10.1016/j.jclepro.2022.135701](https://doi.org/10.1016/j.jclepro.2022.135701).
- Sciara, S., Suk, S.J., Ford, G., 2016. Characterizing Electrical Output of Bifacial Photovoltaic Modules by Altering Reflective Materials, *Journal of Building Construction and Planning Research*, 4, 41-55, doi:10.4236/jbcpr.2016.41003.
- Stein, J., Reise C., Castro, J., Friesen, G., Maugeri, G., Urrejola, E., Ranta, S., 2021. Bifacial Photovoltaic Modules and Systems: Experience and Results from International Research and Pilot Applications. Sandia National Laboratories (SNL), Apr. 2021. Doi: 10.2172/1779379.
- Sultan Mahmud, M., Wazedur Rahman, M., Hossain Lipu, M.S., Al Mamun, A., Annur, T., Mazharul Islam, M., 2018. Solar Highway in Bangladesh Using Bifacial PV. 2018 IEEE international conference on system, computation, automation and networking (ICSCAN), Pondicherry, India, 6-7 July 2018, pp. 1-7, doi: 10.1109/ICSCAN.2018.8541253.